FACTA UNIVERSITATIS
Series: Architecture and Civil Engineering Vol. 21, Nº 3, 2023, pp. 445-471
https://doi.org/10.2298/FUACE231107046M

Original Scientific Paper

ADOPTING A FIBER MACROELEMENT FOR ACCOUNTING THE SSI EFFECT IN NONLINEAR SEISMIC ANALYSIS

UDC 624.131.55
624.042.7

Nikolay Y. Milev

Department of Geotechnics, University of Architecture, Civil Engineering and Geodesy (UACEG), Sofia, Bulgaria

Abstract. *The main purpose of this paper is to propose a practical approach for considering the soil – shallow foundation – superstructure interaction effect in nonlinear seismic analysis. Soil structure interaction is a complicated task dealing with various engineering problems. Taking into account the soil structure interaction extends beyond the numerical analysis, geotechnical investigation, or structural design fields. The artistry of considering the soil structure interaction effect lies in the balance between incorporating soil conditions and the superstructure into one collective model. Following this methodology alongside classical soil mechanics principles provides additional confidence to the structural engineering society in adopting a complete practical concept. The herein presented study introduces a fiber macroelement that represents the soil beneath shallow foundations. This allows for the direct utilization of the fiber macroelement in nonlinear pushover and dynamic analysis in commercial software, as well as its simple implementation in open software systems. The introduction of a procedure for forming the stiffness matrix of the element and a hysteresis soil model is also a key component. Special attention is devoted to obtaining the material backbone curve through experimental results and Eurocode 8's procedures. Furthermore, this paper demonstrates the implementation of a macroelement for considering the soil-structure interaction effect in nonlinear seismic analysis within commercial software. The primary aim is to provide structural designers with a streamlined approach for incorporating soil conditions into superstructure analysis. Numerical analysis results from an example building with a reinforced concrete structure in commercial software highlight the significance of not underestimating soil conditions. This work emphasizes that relying solely on fixed models in everyday structural design could lead to dangerous and unexpected consequences.*

Key words: *macromodel, fiber element, soil structure interaction, soil dynamics, liquefaction, backbone curve of soil, stiffness degradation, hysteresis model, Eurocode 8*

Received November 7, 2023 / Revised November 15, 2023 / Accepted November 16, 2023
Corresponding author: Nikolay Y. Milev, Department of Geotechnics, University of Architecture, Civil Engineering and Geodesy (UACEG), Sofia, Bulgaria
e-mail: milev_fte@uacg.bg

1. INTRODUCTION

In the realm of seismic structural design, the consideration of soil-structure interaction holds a pivotal role. This facet necessitates a nuanced understanding of both components at play – the underlying soil and the superstructure above. Striking the right balance, however, is an intricate challenge; models devised by engineers should be sufficiently sophisticated to capture the nuances of soil-structure interaction, yet not overly complex to hinder practical nonlinear pushover and dynamic analyses. In this paper, we introduce a macromodel designed to represent the behavior of soil beneath shallow foundations. What distinguishes this macromodel is its seamless integration into nonlinear pushover and dynamic analyses, readily applicable within commercial software platforms such as ETABS and SAP2000, while maintaining straightforward implementation in open-source systems like OpenSees and Ruaumoko. This innovative macromodel embodies a harmonious compromise between the inevitable intricacies of modeling soil-structure interaction and the imperative simplicity demanded by routine dynamic nonlinear analyses in structural design practice.

2. DESCRIPTION OF THE FIBER MACROELEMENT

The proposed herein macroelement represents the soil beneath arbitrarily shaped shallow foundations by means of macromodel based on vertical fiber elements – Fig. 2. During the last few decades such kind of finite elements are applied in reinforced concrete structures research. Finite fiber elements for studying of reinforced concrete structures are implemented in commercial software like ETABS as well as in programs with research purposes like DRAIN-2DX and DRAIN-3DX, as suggested in [1] and [2].

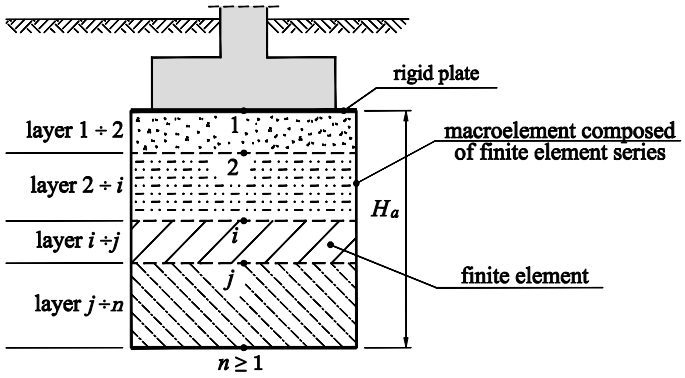

Fig. 1 Macroelement composed of finite fiber elements for modelling the soil structure interaction bellow a spread footing

The studied soil fiber macroelement is located vertically immediately beneath the base of the foundation. The length of the element could be taken as the depth of the affected zone where settlements are generated during seismic excitation. In order to simplify the concept in herein presented research the vertical stress distribution in soil due to lateral stress

effect is taken linearly according to Recommendation for Design of Building Foundations in Japan – [3] (Fig. 2a). This would cause a prismatic shape of the macroelement in all sections – in the base of the foundation and at the end of the affected zone. In order to simplify the implementation of the macroelement in commercial software its cross section is taken constant.

The area of that cross section is taken as the mean value of the area at the base of the foundation and the area at the end of the affected zone (Fig. 2b).

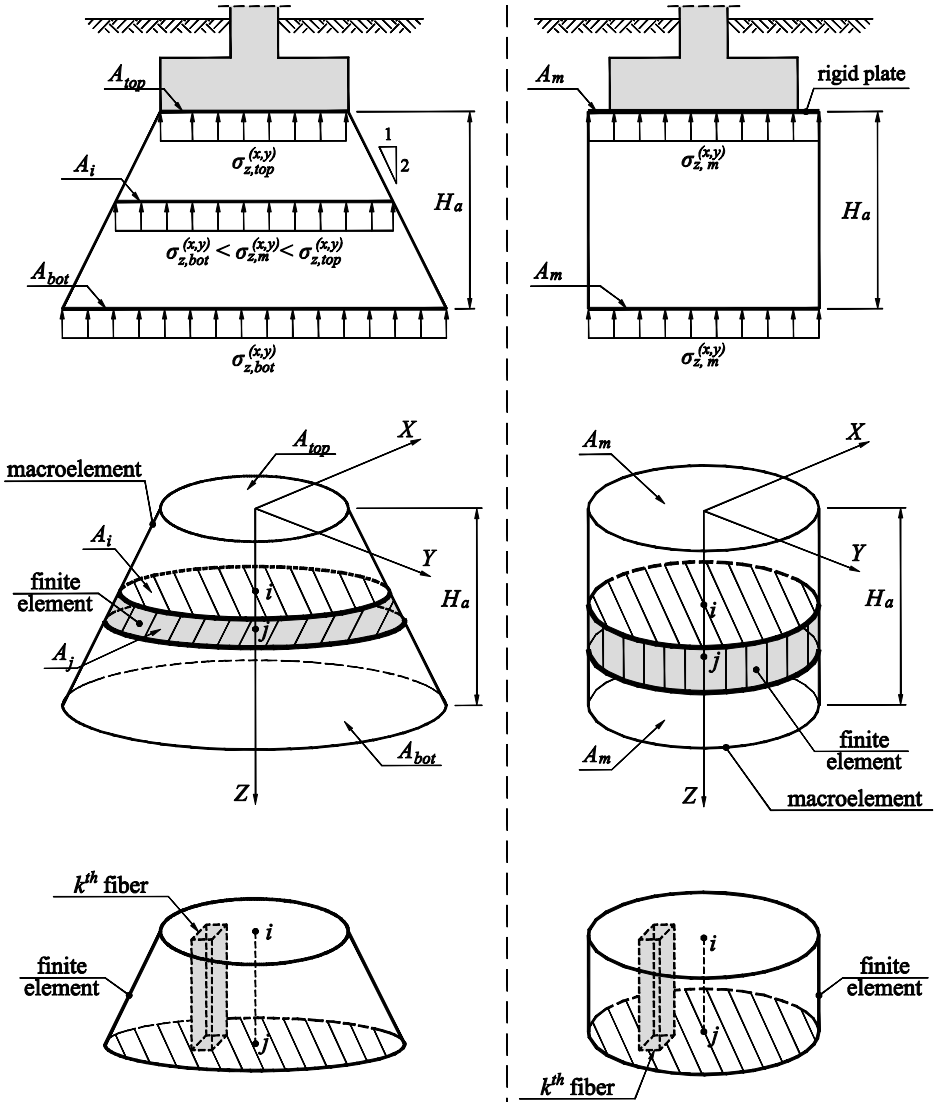

Fig. 2 Fiber macroelement for modelling the soil structure interaction bellow a spread footing based on: a) stress distribution according to Recommendation for Design of Building Foundations in Japan; b) simplified stress distribution

On the other hand, the proposed macroelement could be divided into separate finite elements which are coaxial to the macroelement – Fig. 1 and Fig. 2. This division could be caused by different in-depth soil conditions. Other possible reasons could be unusual loading, the shape of the base and foundation on different levels. All that would possibly lead to division requirement of the macroelement into separate finite elements.

3. FORMING THE STIFFNESS MATRIX OF THE FINITE SOIL FIBER ELEMENT

The fiber element model could be considered as a simplified finite element method which is applied to one-dimensional prismatic element. Each fiber presents a soil element. The nonlinear "stress-strain" relation is assigned to each fiber.

The macroelement and its fiber elements are frame type of finite elements. Furthermore, the following assumptions should be taken into account:

- Axial forces do not interact with the bending moments and shear forces. As a consequence of this they could be defined independently;
- All displacement effects which are perpendicular to the axis of the macroelement are negligible but could be taken into consideration.

The soil finite element is shown in Fig. 3. For the case of nonlinear analysis, the increment of the generalized joint forces $\{\Delta f\}$ and displacements $\{\Delta u\}$ in both ends of the element are given by the following vectors:

$$\{\Delta f\} = \begin{Bmatrix} \Delta M_{x,i} \\ \Delta M_{y,i} \\ \Delta M_{x,j} \\ \Delta M_{y,j} \\ \Delta N_{ij} \end{Bmatrix} \text{ and } \{\Delta u\} = \begin{Bmatrix} \Delta \theta_{x,i} \\ \Delta \theta_{y,i} \\ \Delta \theta_{x,j} \\ \Delta \theta_{y,j} \\ \Delta \varepsilon_{0,ij} \end{Bmatrix} \tag{1}$$

These increments are related by means of the tangent stiffness matrix of the element $[k_m^t]$ by the following equation:

$$\{\Delta f\} = [k_m^t]\{\Delta u\} \text{ or } \begin{Bmatrix} \Delta M_{x,i} \\ \Delta M_{y,i} \\ \Delta M_{x,j} \\ \Delta M_{y,j} \\ \Delta N_{ij} \end{Bmatrix} = \begin{bmatrix} k_{11,m}^t & k_{12,m}^t & k_{13,m}^t & k_{14,m}^t & k_{15,m}^t \\ k_{21,m}^t & k_{22,m}^t & k_{23,m}^t & k_{24,m}^t & k_{25,m}^t \\ k_{31,m}^t & k_{32,m}^t & k_{33,m}^t & k_{34,m}^t & k_{35,m}^t \\ k_{41,m}^t & k_{42,m}^t & k_{43,m}^t & k_{44,m}^t & k_{45,m}^t \\ k_{51,m}^t & k_{52,m}^t & k_{53,m}^t & k_{54,m}^t & k_{55,m}^t \end{bmatrix} \begin{Bmatrix} \Delta \theta_{x,i} \\ \Delta \theta_{y,i} \\ \Delta \theta_{x,j} \\ \Delta \theta_{y,j} \\ \Delta \varepsilon_{0,ij} \end{Bmatrix} \tag{2}$$

In condition that the axial force is constant within the element and the bending moments about axis x and y alter linearly the relation between the increment of the generalized joint forces $\{\Delta f\}$ and the increment of the internal forces $\{\Delta s\}$ in any section could be given as:

$$\{\Delta s\} = [T_f]\{\Delta f\} \text{ or } \begin{Bmatrix} \Delta M_x(z) \\ \Delta M_y(z) \\ \Delta N(z) \end{Bmatrix} = \begin{bmatrix} \left(\frac{z}{L}-1\right) & 0 & \frac{z}{L} & 0 & 0 \\ 0 & \left(\frac{z}{L}-1\right) & 0 & \frac{z}{L} & 0 \\ 0 & 0 & 0 & 0 & 1 \end{bmatrix} \begin{Bmatrix} \Delta M_{x,i} \\ \Delta M_{y,i} \\ \Delta M_{x,j} \\ \Delta M_{y,j} \\ \Delta N_{ij} \end{Bmatrix} \quad (3)$$

Subsequently the element is divided into interconnected vertical fibers between the two end sections which are coaxial to the macroelement (Fig. 4). Bernoulli's principle for plain element sections after its deformation is in effect. The rotation along axis x and y and the extension of the element at the center of mass of the section are actually the degrees of freedom of the section.

The plain sections before their deformation remain plan after the deformation (Bernoulli's principle). As a consequence of this principle the axial strain $\varepsilon_z(x,y)$ in a point with coordinates (x,y) is given as a function of the axial strain at the center of mass of the section $\varepsilon_0(z)$ as well as the curvatures $\varphi_x(z)$ and $\varphi_x(z)$ (positive when they act anticlockwise) as follows:

$$\varepsilon_z(x,y) = \varepsilon_0(z) - x\varphi_y(z) + y\varphi_x(z) \quad (4)$$

The corresponding strain increment $\Delta\varepsilon_z(x,y)$ in point with coordinates (x,y) is given as follows:

$$\Delta\varepsilon_z(x,y) = \Delta\varepsilon_0(z) - x\Delta\varphi_y(z) + y\Delta\varphi_x(z) \quad (5)$$

The increment of the tensile stress $\sigma_z(x,y)$ in the fiber is defined by the increment of the strain $\varepsilon_z(x,y)$ in the fiber and the tangent modulus of the soil (in $E^T(x,y)$):

$$\Delta\sigma_z(x,y) = E^T(x,y)\Delta\varepsilon_z(x,y) \quad (6)$$

The corresponding internal force increment $\{\Delta s\}$ in the section is given by the following equation:

$$\{\Delta s\} = \begin{Bmatrix} \Delta M_x(z) \\ \Delta M_y(z) \\ \Delta N(z) \end{Bmatrix} = \begin{Bmatrix} \int_A \Delta\sigma_z(x,y)x dA \\ \int_A \Delta\sigma_z(x,y)y dA \\ \int_A \Delta\sigma_z(x,y)x dA \end{Bmatrix} \quad (7)$$

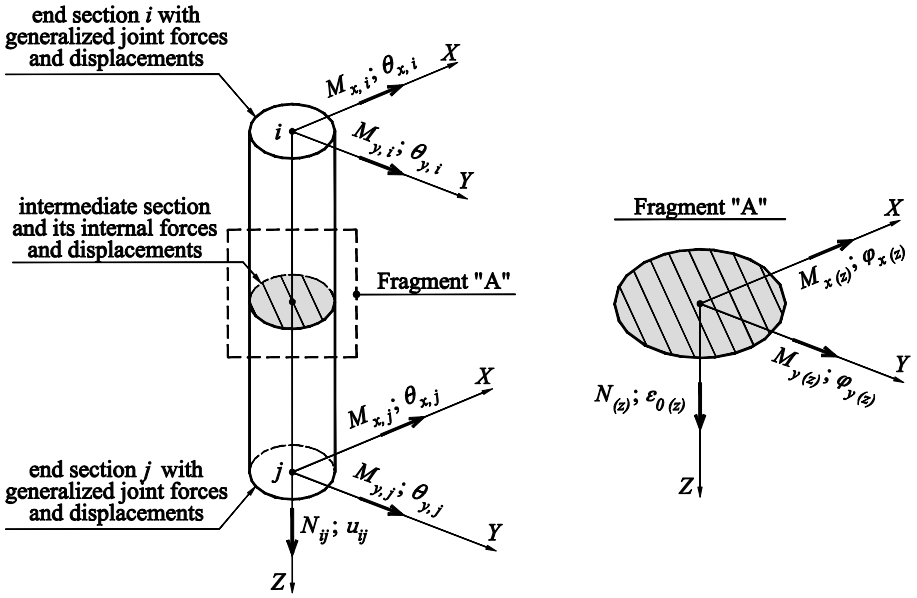

Fig. 3 Generalized joint forces and displacements for a finite element which represents the soil beneath a spread footing

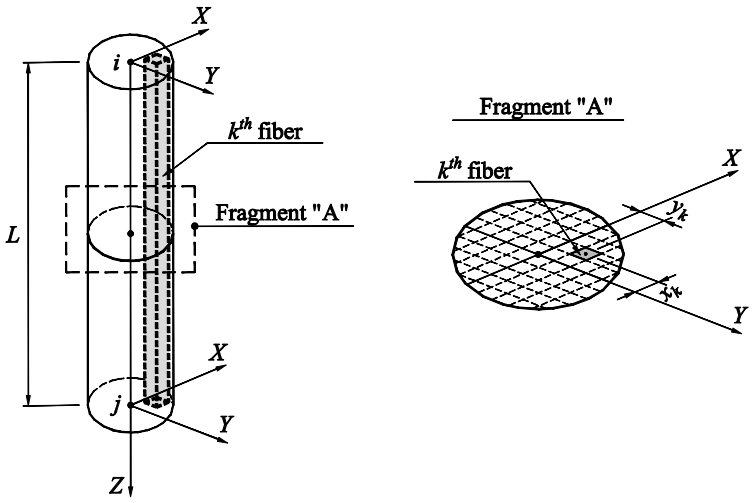

Fig. 4 Fiber finite element for modelling of soil

If equation (5) is substituted in equation (6) and after that equation (6) is substituted in equation (7) and integration is replaced with summation the relation between the internal forces vector increment $\{\Delta s\}$ and the deformation vector increment $\{\Delta d_s\}$ in the section are obtained by means of the tangent stiffness matrix of the section $\{\Delta d_s\}$ as follows:

$$\begin{Bmatrix} \Delta M_x(z) \\ \Delta M_y(z) \\ \Delta N(z) \end{Bmatrix} = \begin{bmatrix} \sum_{kfib=1}^{n} E_{kfib}^T y_{kfib}^2 A_{kfib} & -\sum_{kfib=1}^{n} E_{kfib}^T x_{kfib} y_{kfib} A_{kfib} & \sum_{kfib=1}^{n} E_{kfib}^T y_{kfib} A_{kfib} \\ -\sum_{kfib=1}^{n} E_{kfib}^T x_{kfib} y_{kfib} A_{kfib} & \sum_{kfib=1}^{n} E_{kfib}^T x_{kfib}^2 A_{kfib} & -\sum_{kfib=1}^{n} E_{kfib}^T x_{kfib} A_{kfib} \\ \sum_{kfib=1}^{n} E_{kfib}^T y_{kfib} A_{kfib} & -\sum_{kfib=1}^{n} E_{kfib}^T x_{kfib} A_{kfib} & \sum_{kfib=1}^{n} E_{kfib}^T A_{kfib} \end{bmatrix} \begin{Bmatrix} \Delta\varphi_x(z) \\ \Delta\varphi_y(z) \\ \Delta\varepsilon_0(z) \end{Bmatrix} \quad (8)$$

or

$$\{\Delta s\} = [k_s^t]\{\Delta d_s\} \quad (9)$$

The tangent stiffness matrix of the element $[k_m^t]$ is obtained from the tangent stiffness matrix of the section $[k_s^t]$ as follows:

$$[k_m^t] = \int_0^L [B(z)]^T [k_s^t][B(z)]dz \quad (10)$$

Where: the matrix $[B(z)]$ gives the relation between the deformation increment in the section $\{\Delta d_s(z)\}$ and the generalized displacement increment in the two ends of the element $\{\Delta d_s(z)\}$ as follows:

$$\{\Delta d_s(z)\} = [B(z)]\{\Delta u\} \quad (11)$$

The obtaining of the matrix is rather simple task for prismatic elements with uniform distribution of their stiffness. The matrix is in a relation with the functions of the shape which are chosen for the particular element. In this paper the assumptions proposed in [4] are applied.

4. Obtaining of Material Backbone Curve

This subsection presents a procedure for obtaining of the backbone curve of saturated cohesionless soils with significant pore pressure building during cyclic loading as well as a modification of the method given in [5] for cohesive soils. For this purpose, three parameters of the material should be defined as follows:

- Damping ratio of the material.
- Yielding point.
- Failure point.

An atypical procedure based on experimentally obtained results and classical soil mechanics approaches is proposed for defining those three parameters.

The damping ratio of the material should be evaluated in the first place. According to [6] the strain levels observed during exploitation of shallow foundations is between 0.05% and 0.125%. The damping ratio could be averaged for that range by means of an experimentally obtained damping ratio against logarithm of strains plot. Another possible approach is to define the damping ratio from the same experimentally evaluated curve for particular strain value – the yielding point of the material.

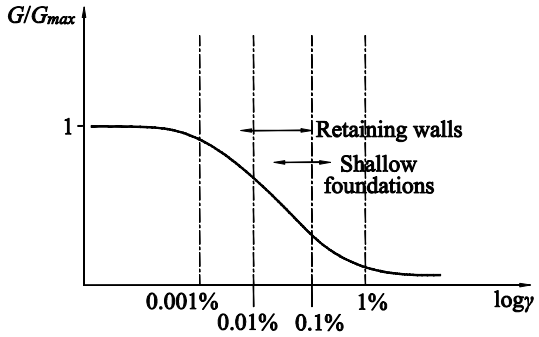

Fig. 5 Stiffness degradation curve of soil and strain levels observed during exploitation of various geotechnical structures

The evaluation of the bearing capacity of saturated cohesionless soils with significant pore pressure building during cyclic loading is not a well-defined topic in *Eurocode 8* [7]. This is the reason why an analogy based on *Eurocode 8*'s (*Annex F*) parameter $\tau_{cy,u}$ (cyclic undrained shear strength) and liquefaction assessment of such kind of soils is made. The liquefaction bearing capacity ($\tau_{cy,u}$) is obtained by means of the normal stress $\sigma_{cy,u}$ (when Poisson's ratio of soil is set as 0.5 for undrained conditions in seismic situation) using a Japanese standard procedure [8] which relates $\tau_{cy,u}$ with a *CSR*-N_c (cyclic stress ratio against number of cycles which cause double amplitude of 5% axial strain during cyclic triaxial tests) curve and the overburden stress as follows:

$$\tau_{cy,u} = CSR_{15}^{tx}.\sigma_{\gamma}^{'}\left[0.9(1+2K_0)\right]/3 \tag{12}$$

where*:*

CSR_{15}^{tx} – cyclic stress ratio for which 15 cycles of loading cause double amplitude of 5% axial strain;

$\sigma_{\gamma}^{'}$ – effective overburden stress,

K_0 – coefficient of earth pressure at rest.

For Poisson's ratio of soil set as 0.5 for undrained conditions in seismic situation the following equation could be given:

$$\sigma_{cy,u} = 2\tau_{cy,u} \tag{13}$$

When the stiffness degradation (Young's modulus against axial strain plot: E_u-ε) of soil is known it is possible to define a "stress-strain" curve of the soil material itself ($\sigma = E_u\varepsilon$) without taking into account the presence of the shallow foundation. The yielding strain ε_y could be defined graphically for $\sigma_{cy,u}$ from the same curve. In order to consider the shape and depth of the foundation a classical approach for evaluating a vertical foundation spring stiffness [9] is used.

During a seismic excitation the foundation spring stiffness value is doubled according to *Design of Highway Bridge Foundations in Japan*. A sloping line is drawn based on thus obtained spring stiffness and interrupted at yielding strain ε_y. Subsequently the yielding stress q_y is obtained graphically for ε_y. From point with coordinates (ε_y ; q_y) a new 10%

sloping line is drawn. An analogy with [10] is made for a failure criterion in which $0.9q_y$ stress gives half of the ultimate strain ($0.5\varepsilon_u$). The 10% sloping line is interrupted at ultimate strain ε_u where the bearing capacity suddenly drops down to 0.1 q_y and the "stress-strain" relation continues parallel to the abscissa (strain axis).

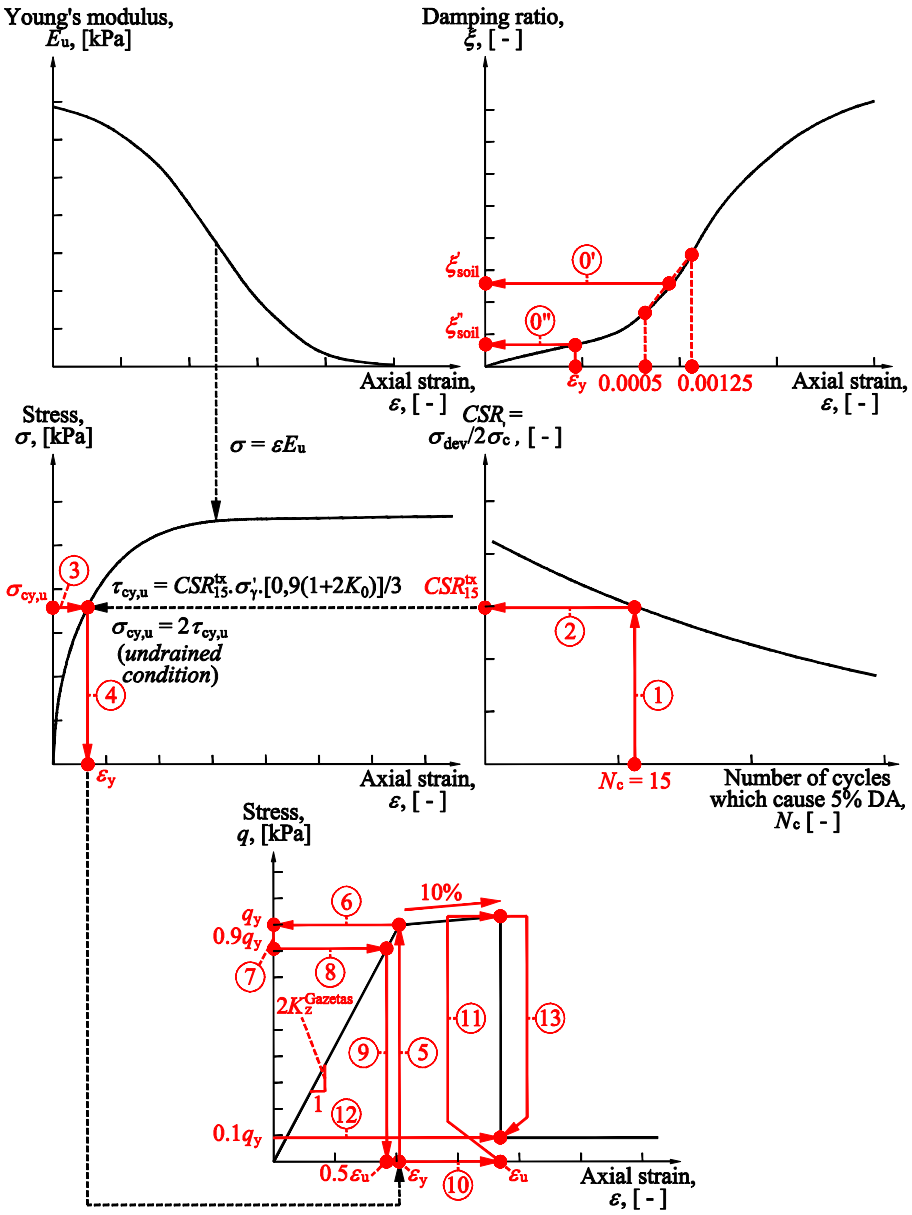

Fig. 6 An approach for backbone curve obtaining for cohesionless soils based on experimental results

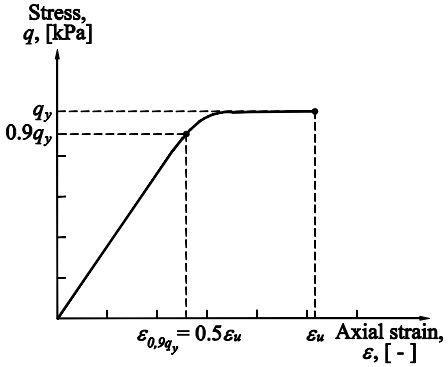

Fig. 7 Shallow foundation failure criterion according to [10]

Modifying the method in [5] the same failure criterion [10] (Fig. 7) is used for defining the failure point with coordinates (ε_u ; q_u) for cohesive soils. The difference in obtaining the backbone curve for cohesive soils is based on the yield stress q_y which is evaluated using the formula for bearing capacity of shallow foundations in undrained conditions given in *Eurocode 8* (*Annex F*) – [7].

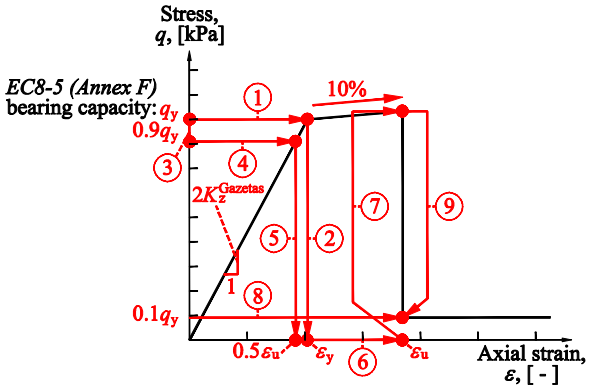

Fig. 8 An approach for backbone curve obtaining for cohesive soils

Fig. 6 presents a summary of the proposed procedure for defining the soil backbone curve based on four experimentally obtained material relations for saturated cohesionless soils with significant pore pressure building during cyclic loading. Similarly, the approach for obtaining the backbone curve of cohesive soils is presented in Fig. 8.

The backbone curves obtained on the basis of experimental investigations which have been performed at the University of Tokyo for Sofia sand and Toyoura sand ([11]: Fig. 9 and Fig. 10) are presented in Fig. 11 as well as the backbone curve of typical Sofia clay (design value of undrained shear strength $c_{u,d}$ of 175 kPa, maximum shear modulus G_{max} of 30 MPa and density ρ_n of 1.88 g/cm^3) which is presented in Fig. 12.

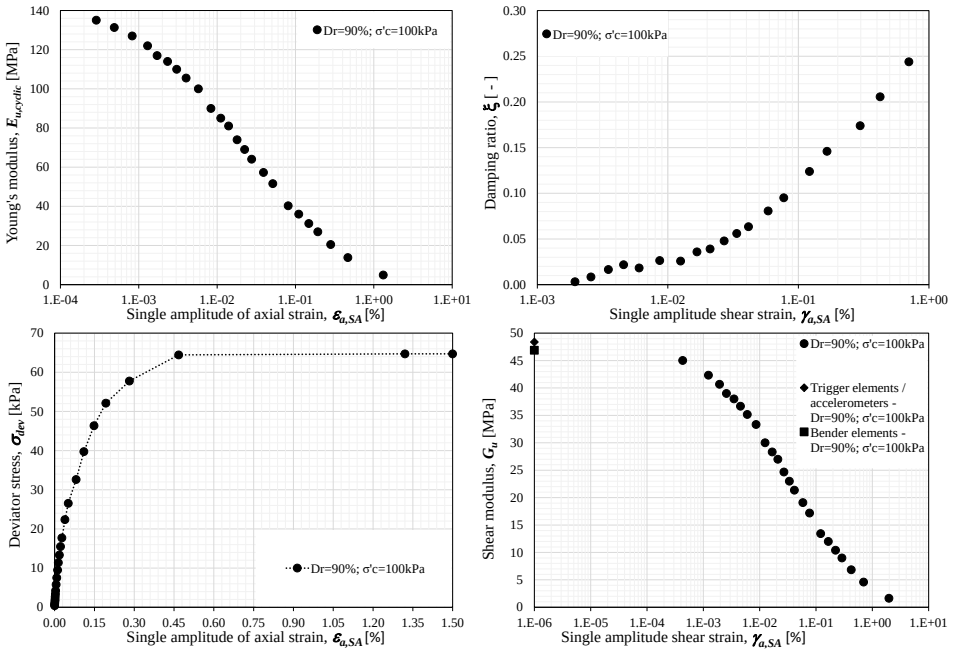

Fig. 9 Experimental evaluation of dynamic soil parameters for Sofia sand

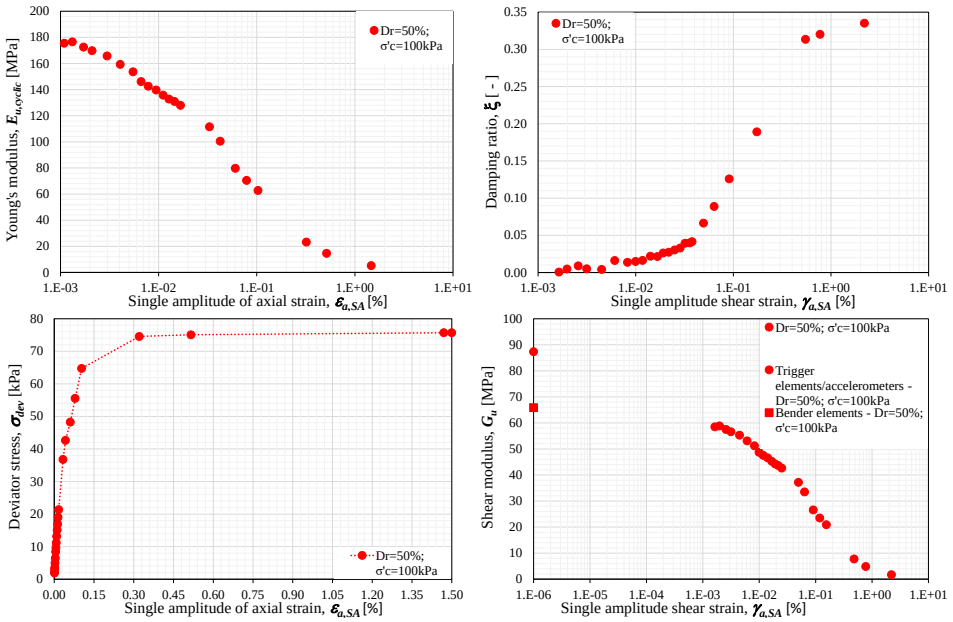

Fig. 10 Experimental evaluation of dynamic soil parameters for Toyoura sand

The foundation spring stiffness [9] is defined for a spread footing (width of 3.0 m, length of 8.5 m, height of 0.5m and foundation depth of 3.0 m) under a shear wall according to [11].

The maximum shear modulus which is required in this procedure [9] is defined using the laboratory determined shear wave velocity of the material ($G_{max} = V_s^2\rho$, where: G_{max} – maximum shear modulus, V_s – shear wave velocity, ρ – soil's density) – Fig. 9 and Fig. 10.

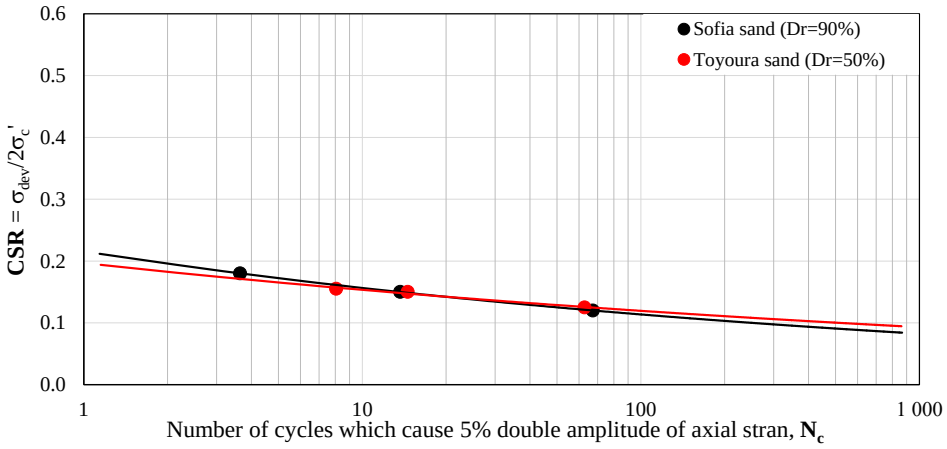

Fig. 11 Experimentally obtained CSR-Nc relations for Sofia sand and Toyoura sand – cyclic triaxial tests

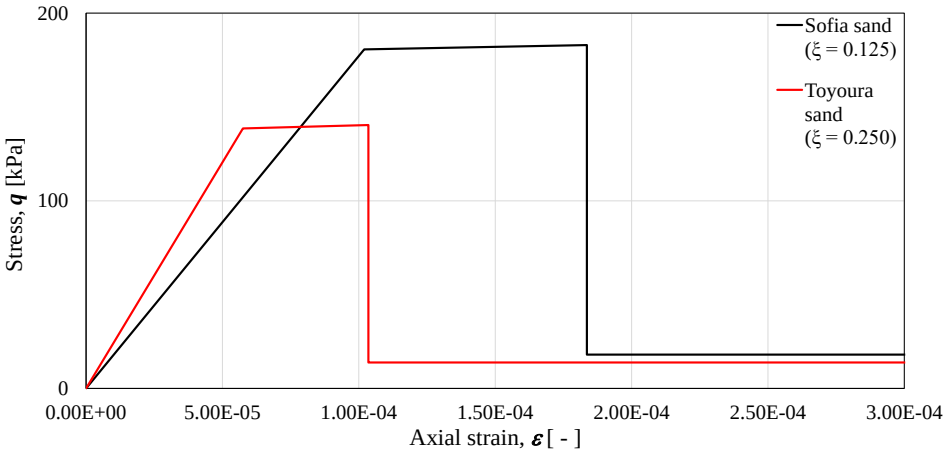

Fig. 12 Backbone curve of cohesionless soils obtained by means of experimental results – procedure according to this study

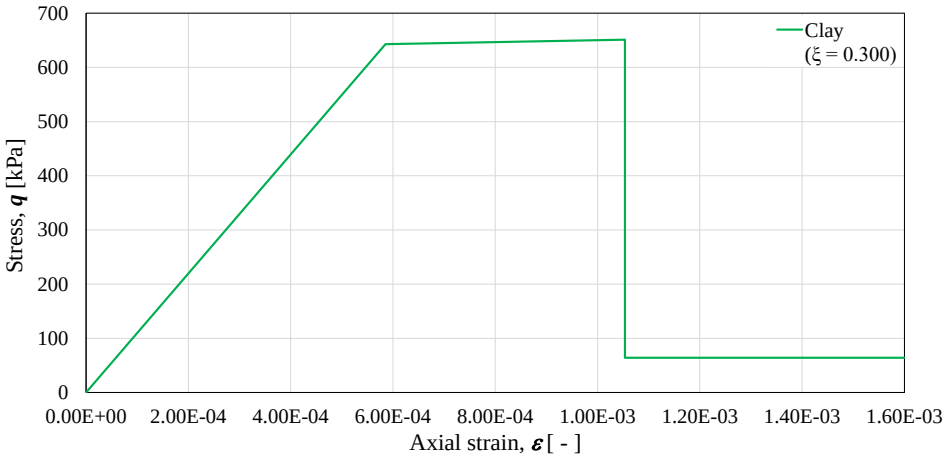

Fig. 13 Backbone curve of cohesive soil obtained by means of bearing capacity of soil according to *Eurocode 8* (*Annex F*) – procedure according to this study

5. SOIL HYSTERESIS MODEL

The hysteresis model which gives the "stress-strain" relation in the soil fiber element is given in Fig. 13. The main assumptions of the model are as follows:

- The algorithm for obtaining the backbone curve of the material is given in previous chapter.
- The material does not bear tensile forces.
- The rules of the hysteresis model are given below.

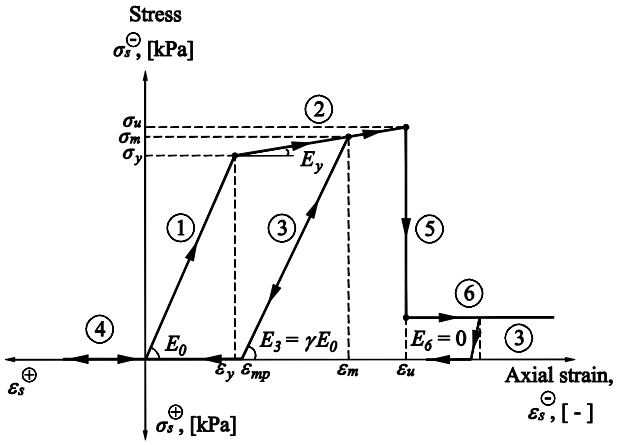

Fig. 14 An approach for backbone curve obtaining based on experimental results

1) *Rule 1*: Elastic response. If $\sigma_i < \sigma_y$, go to *Rule 2*. If $\sigma_i > 0$, go to *Rule 4*. Elastic stiffness: $E_1 = E_0$.
2) *Rule 2*: Yielding along the backbone curve. If $\sigma_i < \sigma_u$, go to *Rule 5*. Yielding stiffness: $E_2 = E_y = \beta E_0$ and $\beta = 0.05 \div 0.10$.
3) *Rule 3*: Unloading and reloading. If $\sigma_i > 0$, go to *Rule 4*. If $\sigma_i < \sigma_m$, go to *Rule 2*. Loading and reloading stiffness: $E_3 = \gamma E_0$ and $0.5 \leq \varepsilon_y / \varepsilon_m \leq 1.0$.
4) *Rule 4*: Tension. $\sigma_i = 0$. If $\varepsilon_i < \varepsilon_{mp}$, go to *Rule 3*. Tension stiffness: $E_4 = 0$.
5) *Rule 5*: Material failure followed by sudden decrease of its bearing capacity. Failure stiffness: $E_5 = 0$.
6) *Rule 6*: Same as *Rule 2*, but the material has failed. Stiffness: $E_6 = 0$.

6. EXAMPLE – PROTOTYPE STRUCTURE AND SOIL

The suggested application of a fiber macroelement in commercial software is based on a prototype building presented in [12]. The building consists of a frame structure with two reinforced concrete walls in transverse direction. The foundation structure is formed by spread footings beneath the columns which are combined by foundation beams. Two additional strip footings are considered beneath the reinforced concrete walls. A spatial view and section of the building as well as a formwork plan of the foundations are given in Fig. 15 ÷ Fig 17.

Two numerical models which differ from each other by the soil conditions which are considered below the foundation structure have been developed independently. One has adopted the laboratory obtained soil parameters of cohesionless soil (Sofia sand) [11], Table 1, and the other is based on cohesive soil with typical parameters of Sofia clay (Table 2).

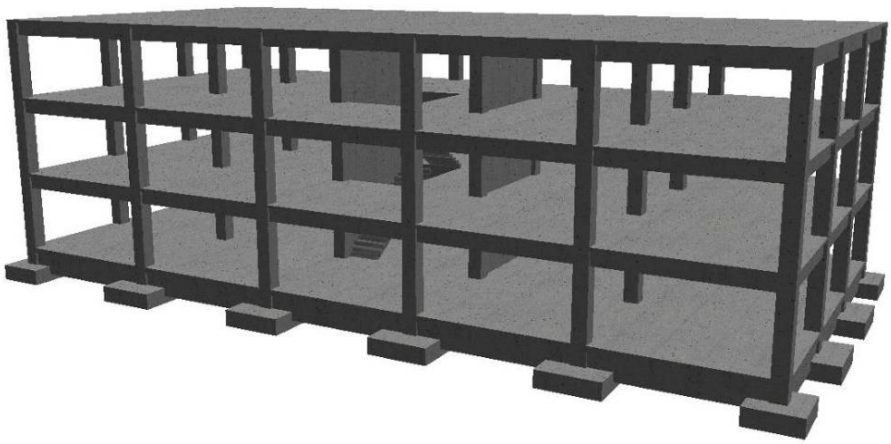

Fig. 15 Spatial view of the prototype structure [12]

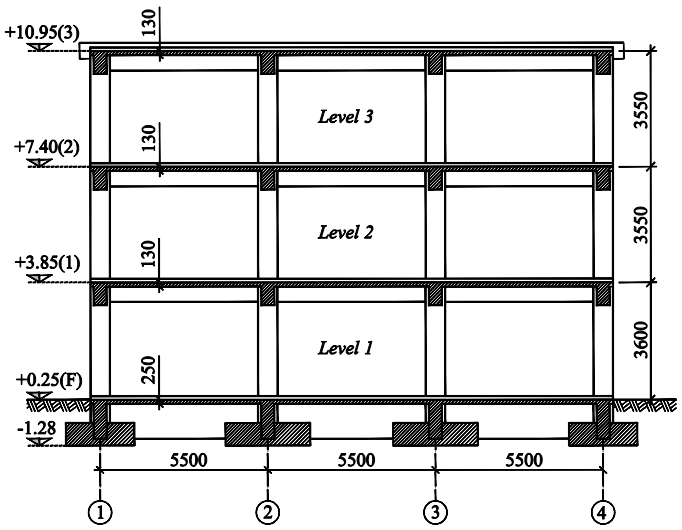

Fig. 16 Section of the prototype structure [12]

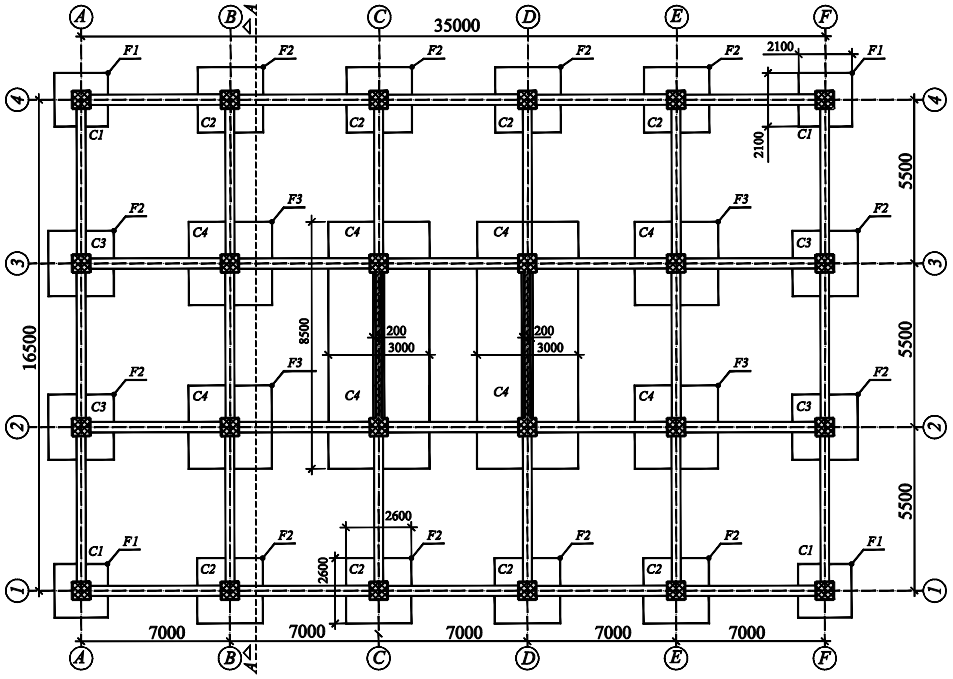

Fig. 17 Formwork plan of the foundation structure of the prototype structure [12]

The strip foundations below the reinforced concrete walls have width, B, of 3.0 m, length, L, of 8.5 m and height, h_f, of 0.50 m. A 3.0 m embedment depth, D_f, of the whole foundation structure has been set. The vertical design load at the base of each strip

footing is 3 652 kN. The bearing capacity of the strip footings under only vertical loading, $R_{v,d}$, has been estimated as well – 46 798 kN for the case of sand and 8 440 kN for the case of clay. Hence the safety factor, $N = R_{v,d} / N^{f}_{ed}$, for both types of soil is estimated as 12.81 and 2.31 respectively.

Table 1 Experimentally evaluated parameters for saturated Sofia sand [11]

Specific density	Dry density	Void ratio	Max. void ratio	Min. void ration	Relative density	Mean particle diameter	Fines content	Coef. of unif.	Angle of Intr. Fric.
ρ_s	ρ_d	e	e_{max}	e_{min}	D_r	D_{50}	F_C	C_U	φ
[g/cm^3]	[g/cm^3]	[-]	[-]	[-]	[%]	[mm]	[%]	[-]	[^{o}]
2.68	1.40	0.918	1.390	0.866	90	0.22	4.24	2.19	38.46

Table 2 Parameters adopted for Sofia clay

Natural density	Cohesion	Angle of Intr. Fric.	Undrained strength	Initial shear modulus
ρ_n	c'_d	φ'_d	$c_{u,d}$	G_{max}
[g/cm^3]	[-]	[^{o}]	[kPa]	[MPa]
1.88	18.30	17.80	105	30

7. NUMERICAL MODELLING

Three spatial numerical models of the structure have been developed in commercial software (ETABS 2015 v. 2.2 – [13]) for cohesive and cohesionless soil conditions (Sofia sand and Sofia clay).

The first model treats Sofia sand as elastic material and the second one considers its elastic-plastic behavior. The third model has been developed in order to capture the elastic-plastic behavior of Sofia clay. Plastic hinges have been defined in the frame joints of the superstructure in order to take into consideration its nonlinearity during seismic action. The reinforcement of the columns and beams has been adopted according to [12]. Fig. 18 represents a spatial view of the numerical models.

The interaction between the structure and the soil beneath the reinforced concrete walls is represented nonlinearly by means of a fiber macroelement (for the case of the numerical models which consider cohesive and cohesionless soil conditions) and linearly by bed of springs (only for the case of the numerical model which considers cohesive soil conditions). The bed of springs' stiffness is evaluated according to *FEMA 356* [14] and its value in the end zones along the longitudinal direction of the strip footing [min(B_x;B_y)/6 = 0.5 m] has been increased. The following bed of springs stiffness has been estimated: k_{end} = 656 500 kN/m/m in the end zones and k_{mid} = 70 100 kN/m/m in the middle zone. The springs themselves have been defined as compression only springs in order to capture the foundation uplifting phenomena in the analysis.

The soil beneath each of the column's spread footings has been represented by two orthogonal horizontal springs and one vertical spring according to [9].

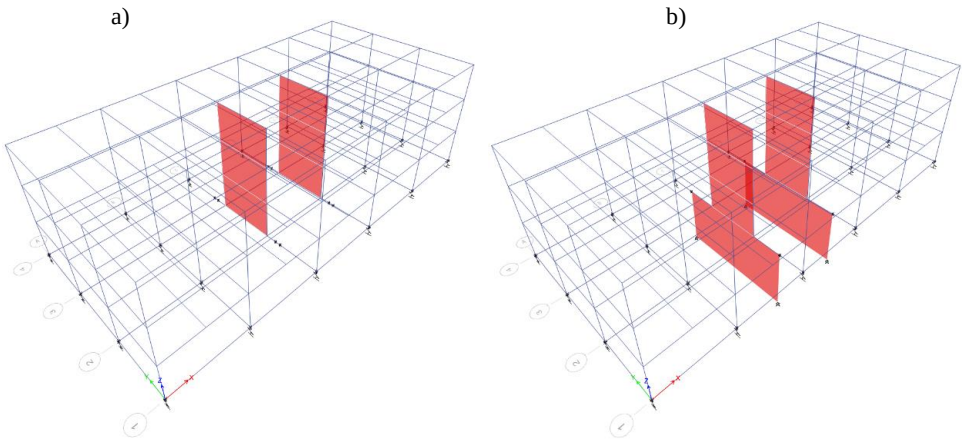

Fig. 18 Spatial model in ETABS: a) elastically supported (compression springs according to FEMA 356); b) fiber element

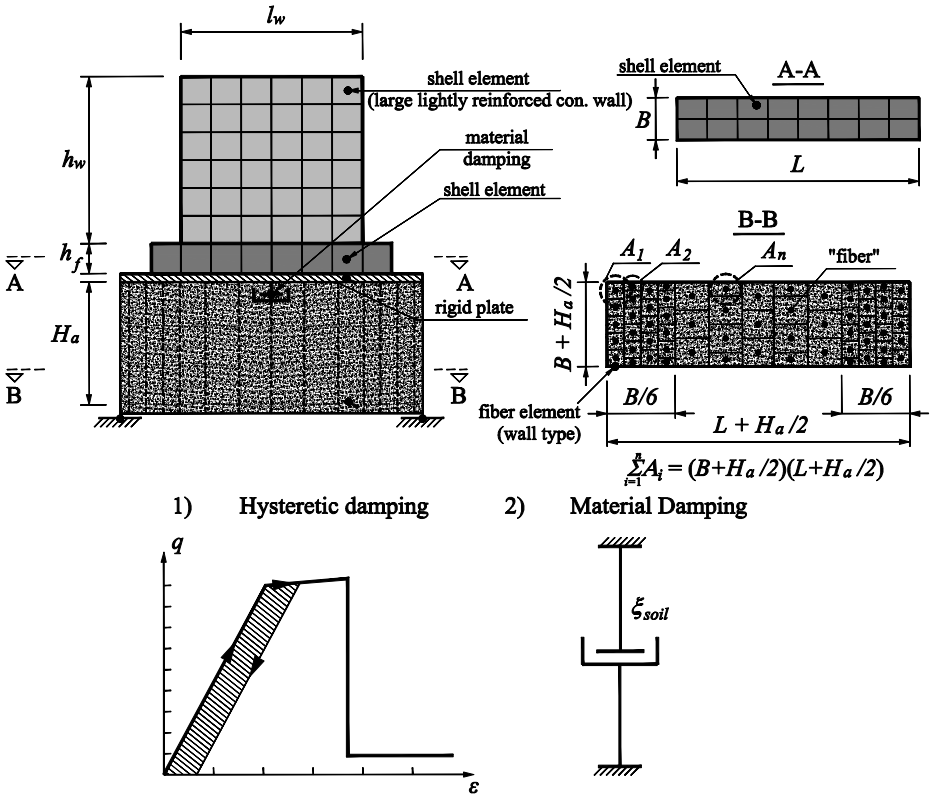

Fig. 19 Schematic representation of rocking foundations by means of macroelements in the software ETABS

Depending on the soil conditions and spread footings' dimensions the following values have been estimated: $K_{z(2.1x2.1m)}$ = 718 000 kN/m, $K_{z(2.6x2.6m)}$ = 830 000 kN/m and $K_{z(3.0x3.0m)}$ = 919 000 kN/m for the numerical models based on Sofia sand and $K_{z(2.1x2.1m)}$ = 445 000 kN/m, $K_{z(2.6x2.6m)}$ = 514 000 kN/m and $K_{z(3.0x3.0m)}$ = 570 000 kN/m for numerical model based on Sofia clay.

The idealization of the prototype structure has been performed by means of the library built-in elements of ETABS 2015 (v. 2.2) – Fig. 18: frame elements for the columns and beams, shell elements for the walls and slabs, plastic hinges for the frame joints of the superstructure and springs for the bottom end of the vertical structural elements.

On the one hand the reinforced concrete walls which have been represented by shell elements transfer the seismic effect to the soil through a rigid plate. On the other hand, the soil and the strip footings are represented by fiber elements whose height is the affected zone beneath the foundations in seismic design combination – H_a.

The fiber element has constant dimensions of the cross section through its whole height. The area of the cross section is the mean value of the cross-section's area immediately beneath the foundation (strip footing's area) and the cross-section's area at the bottom end of the affected zone – in other words an addition of $H_a/2$ to each strip foundation side forms the perimeter of the fiber element (Fig. 19). The backbone curve of the material (soil) has been obtained by means of the procedure given in [11].

The procedure for defining the soil fiber element in ETABS 2015 as well as the fiber distribution in the cross section are shown in Fig. 20. Each fiber is characterized by its coordinates, material type and area (A_{fiber} = 690 000 cm^2).

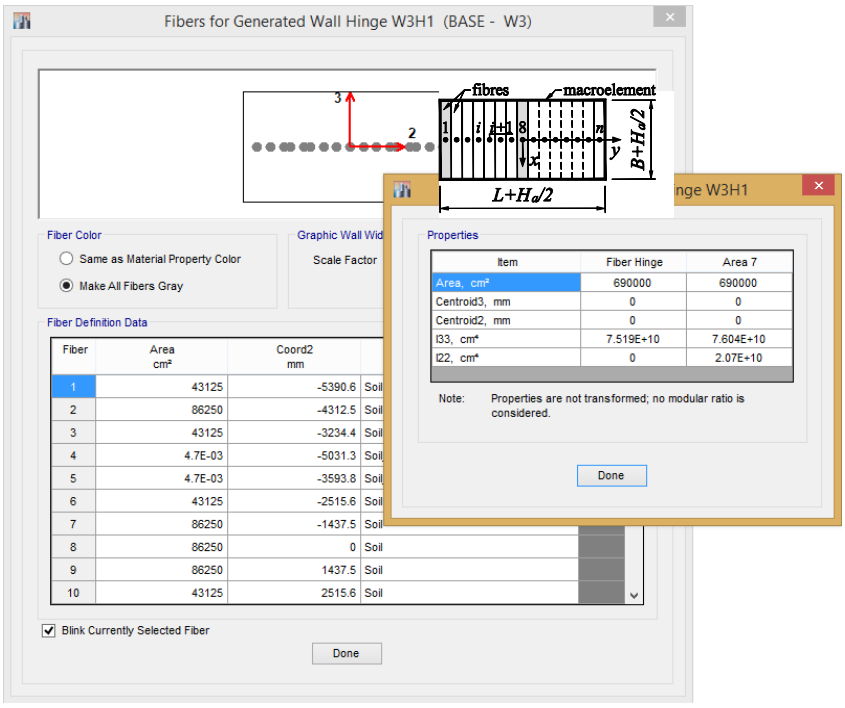

Fig. 20 Formwork plan of the foundation structure of the prototype structure [12]

A spatial view of the numerical model of the prototype structure is shown in Fig. 21.

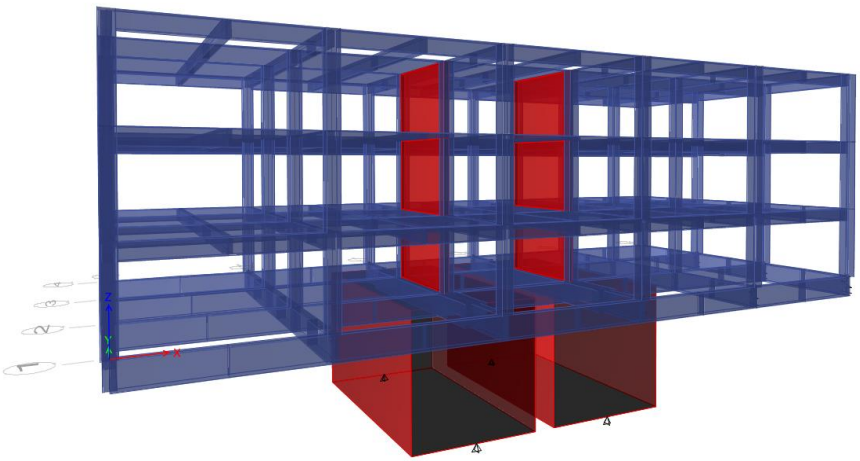

Fig. 21 Spatial view of the prototype structure in ETABS

The behavior of the prototype structure during seismic excitation has been studied by nonlinear time-history analysis. The implemented accelerogram (North-South record) is taken from the El Centro earthquake from 1940 (PGA = 3.4 m/s^2 = 0.34g). The dynamic excitation is defined along global axis Y only – the direction of the reinforced concrete walls. The record has been scaled gradually in increasing sense for different values of the peak ground acceleration – PGA. The main purpose to do so is to study the prototype structure performance during seismic action of various magnitude. The adopted accelerogram (North-South record) from the El Centro earthquake is shown in Fig. 22.

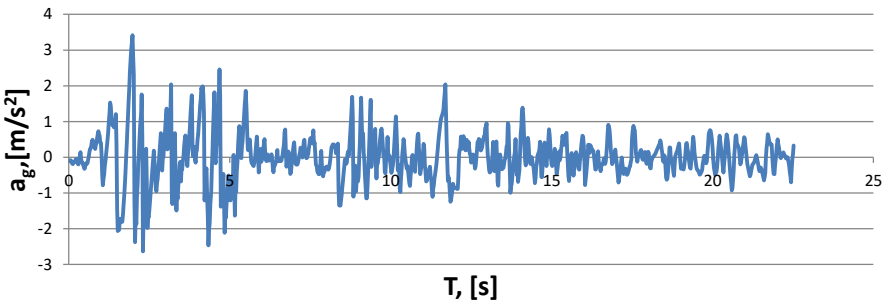

Fig. 22 Accelerogram (North-South) from the El Centro earthquake (1940) (PGA = 3.4 m/s2) used in the nonlinear time-history analysis

8. Results and Discussion

At first the seismic performance of the prototype structure taking into consideration the interaction with cohesionless soil with significant pore pressure building during cyclic loading (Sofia sand) has been studied. The results (Fig. 23 and Fig.

24) show that the soil behaves linearly up to *PGA* = 0.20*g* and at *PGA* = 0.30*g* its bearing capacity is mobilized.

The moment-rotation relation of the fiber element as well as the stress-strain relation of the most severely loaded (outermost) fiber (Fiber 1 – Fig. 19) for various values of *PGA* are shown in Fig. 25.

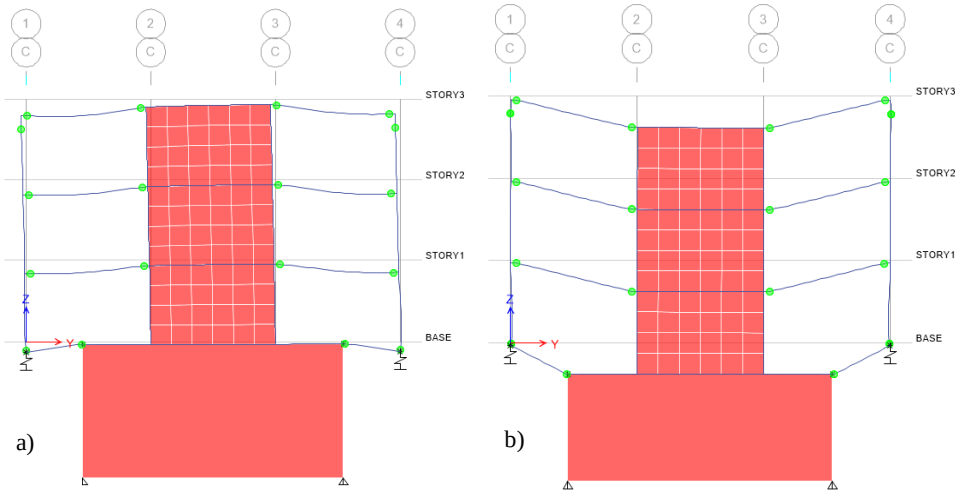

Fig. 23 Model with Sofia sand soil conditions: section of the prototype structure under seismic excitation of: a) PGA = 0.20*g*; b) PGA = 0.30*g*

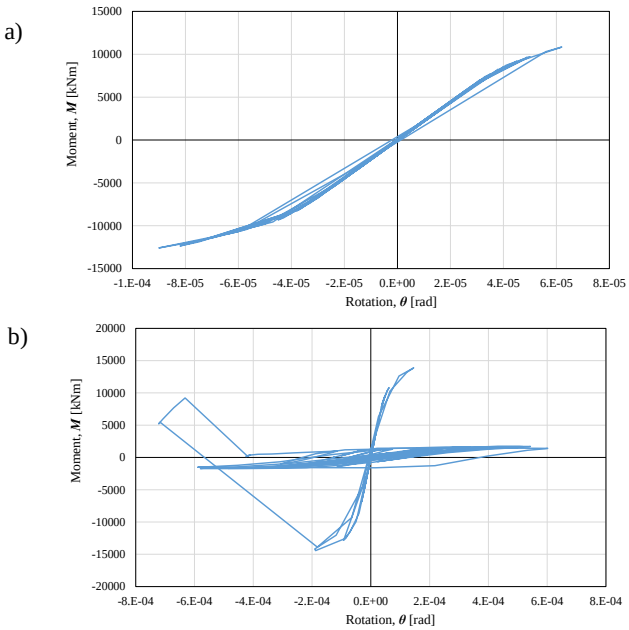

Fig. 24 Sofia sand: "Moment-Rotation" relation in time in the fiber element for: a) PGA = 0.20*g*; b) PGA = 0.30*g*

The performance of the superstructure remains elastic during the whole loading range up to PGA = 0.30g (Fig. 26). Oversimplification or total ignoring of the interaction between soil and structure in seismic analysis of buildings is a common approach of structural designers.

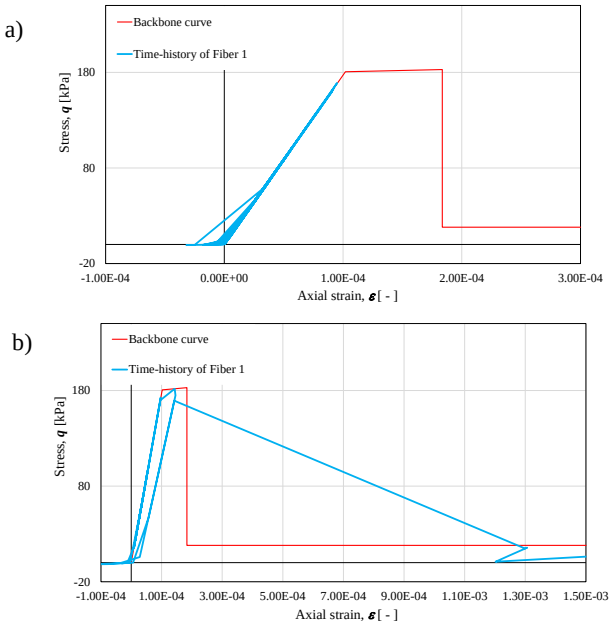

Fig. 25 Sofia sand: "Stress-Strain" relation in time in Fiber 1 of the element for: a) PGA = 0.20*g*; b) PGA = 0.30*g*

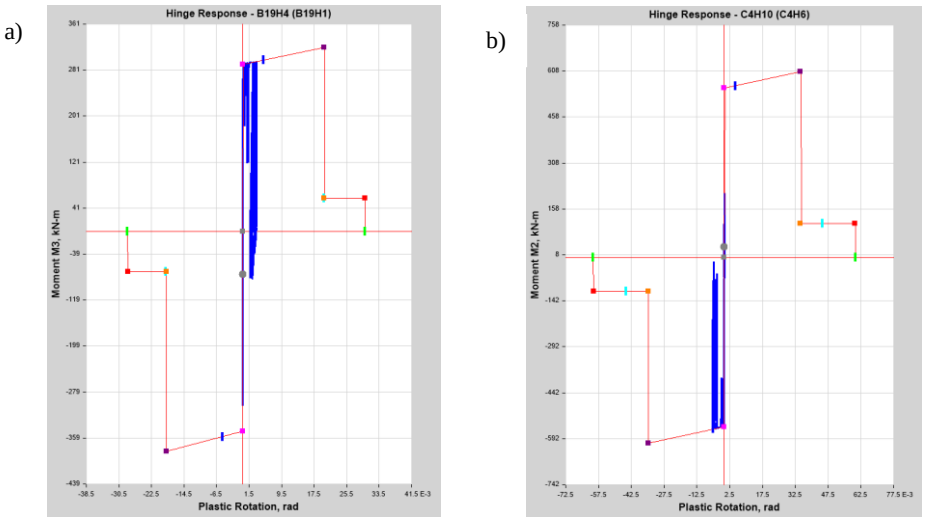

Fig. 26 Sofia sand: "Moment-Rotation" relation in time in "Column-Beam" joint of the frame RC structure of the prototype structure for PGA = 0.30*g*: a) beam G8; b) column C4

The results from the analysis are usually obtained from the premise that the model is fixed at the base of the structure which underestimates the fact that under some conditions the soil fails way before the seismic energy dissipating structural elements (shear walls or frame beams and columns). This concept could lead to totally false understanding of the overall performance of the soil – foundation – superstructure system during design seismic excitation. Such phenomenon is demonstrated in the nonlinear analysis by taking into account the soil conditions' influence on the superstructure. The soil – foundation system is represented simultaneously by fiber macroelements and a bed of springs (Fig. 27).

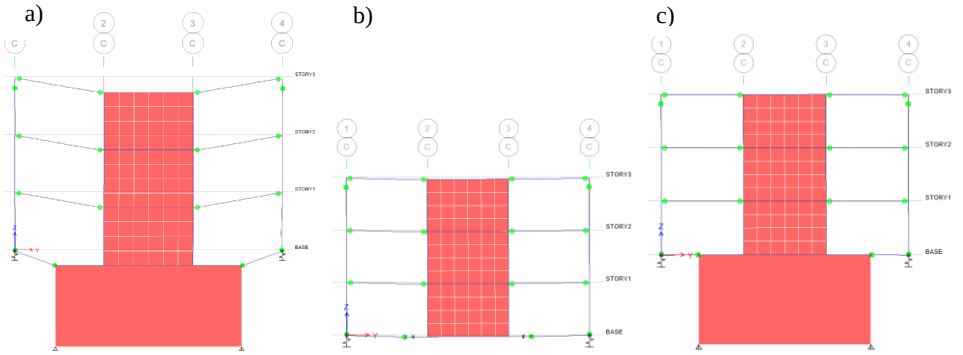

Fig. 27 Section showing the response of the prototype structure for PGA = 0.30*g* for various types of models and soil conditions: a) Sofia sand: macroelement fiber model; b) Sofia sand: elastically supported (spring) model according to FEMA 356; c) Sofia clay: macroelement fiber model

The results from the seismic analysis (Fig. 27) show that the fixed value of *PGA* (0.30*g*) for various soil conditions and various approaches for consideration of the soil – structure interaction leads to significantly different response of the soil – shallow foundation – superstructure system. Although the safety factor in static condition, *N*, has a considerably higher value for spread footings in saturated Sofia sand (N = 12.81) compared to the one of spread footings in Sofia clay (N = 2.31) the overall response of the system in the latter soil conditions is more favorable. This conclusion confirms the statement that saturated cohesionless soils with significant pore pressure building during cyclic loading are vulnerable during major earthquakes.

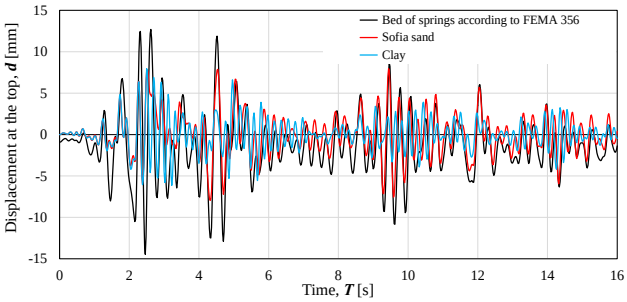

Fig. 28 Displacement history in time at the top of the prototype structure for PGA = 0.30*g* for various types of models and soil conditions

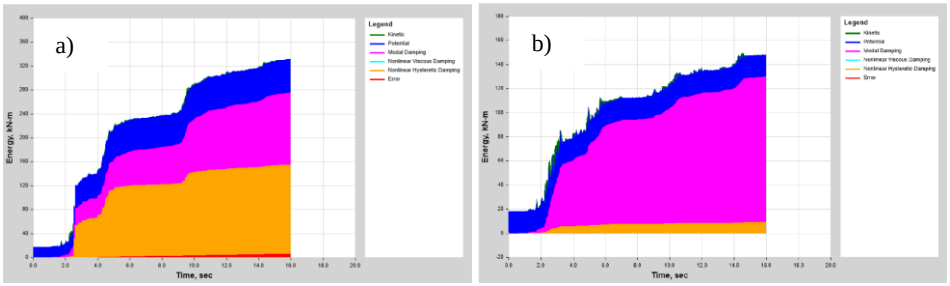

Fig. 29 Energy history in time in the prototype structure for PGA = 0.30*g*: a) Sofia sand; b) Sofia clay

Fig. 30 Settlement due to soil failure – Kocaeli (Turkey) earthquake (1999)

In contrast with the fiber macroelement model the elastically supported (springs) model with Sofia sand soil conditions is not capable of capturing the stiffness degradation (liquefaction) of soil. Fig. 28 shows a comparison of the displacement time-history of a point at the top of the superstructure. The diagram confirms the statement that different soil conditions and different type of models lead to different behavior of the superstructure.

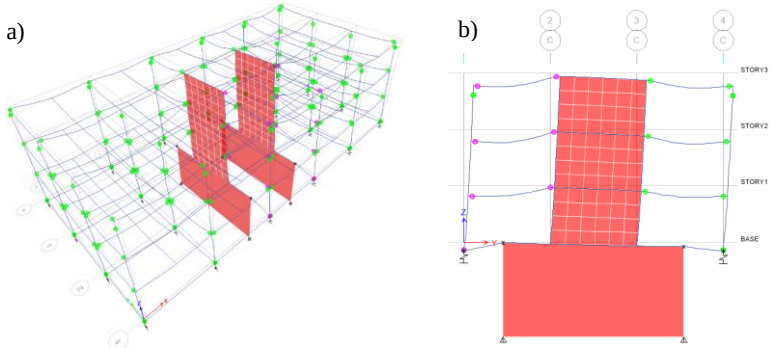

Fig. 31 Sofia clay: response of the prototype structure for PGA = 1.5*g*: a) spatial view; b) section

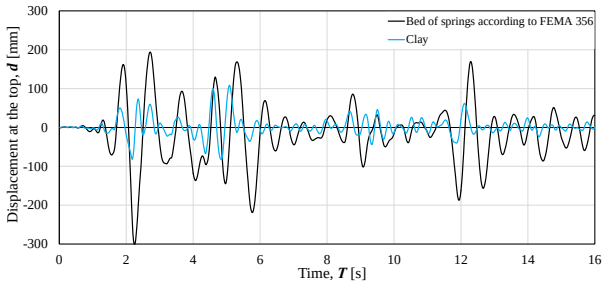

Fig. 32 Sofia clay: displacement history at the top of the prototype structure for PGA = 1.5*g* for various types of models

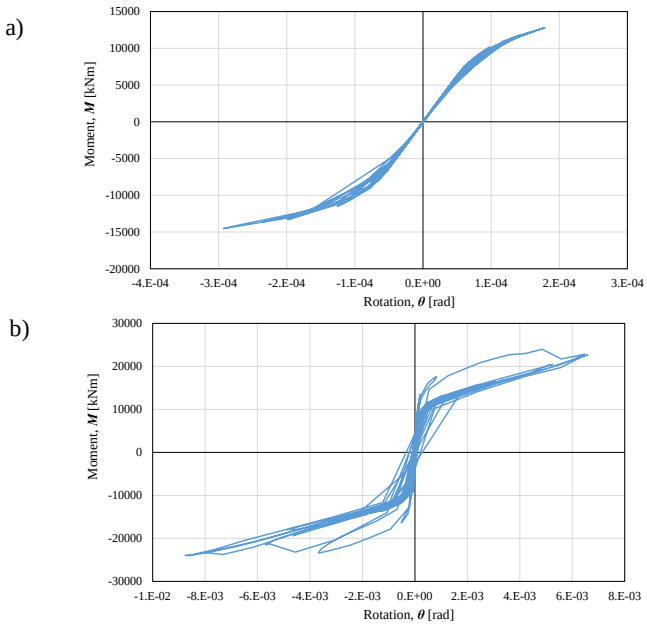

Fig. 33 Sofia clay: "Moment-Rotation" relation in time in the fiber element for: a) PGA = 0.30*g*; b) PGA = 1.50*g*

Larger displacements are observed in the elastically supported (spring) model. As it could be seen in Fig. 29 the energy time-history for PGA = 0.30 differs mostly in terms of nonlinear hysteresis energy. The energy is observed to be more in Sofia sand soil conditions than in Sofia clay soil conditions.

From a historical point of view the problem with cohesionless soil with significant pore pressure building during cyclic loading is well known. Fig. 30 shows a photograph of building after the Kocaeli (Turkey) earthquake from 1999. Its superstructure is unharmed but a considerable settlement is observed in the foundations probably due to liquefaction. In order to demonstrate the importance of the soil conditions (captured by the input backbone curve) the results from a macroelement fiber model with clay has been presented (Fig. 31).

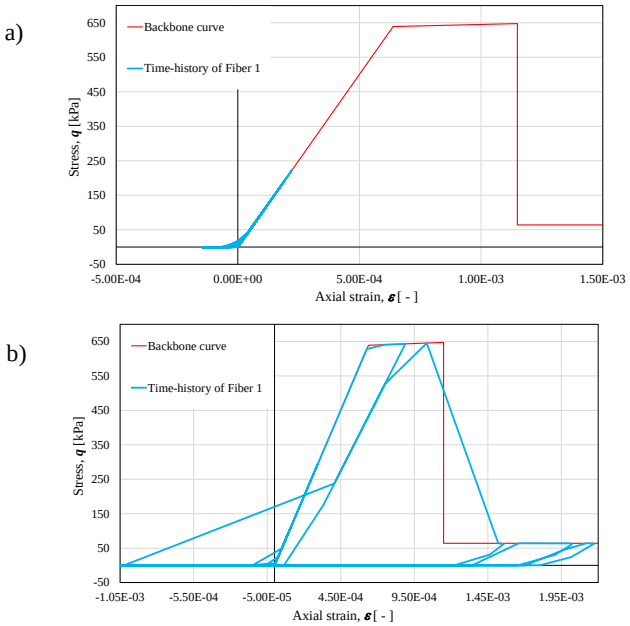

Fig. 34 Sofia clay: "Stress-Strain" relation in time in Fiber 1 of the element for: a) PGA = 0.30*g*; b) PGA = 1.50*g*

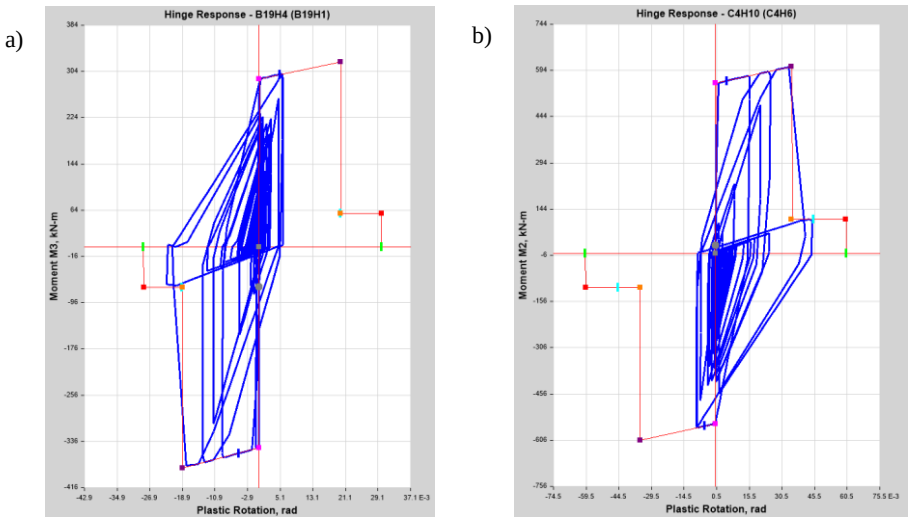

Fig. 35 Sofia clay: "Moment-Rotation" relation in time in "Column-Beam" joint of the frame RC structure of the prototype structure for PGA = 1.50*g*: a) beam G8; b) column C4

The results show that in such soil conditions the system formally yields at *PGA* = 0.90*g* and fails at *PGA* = 1.50*g*. Relatively high values of *PGA* (such as 0.90*g* and 1.50*g*) show significant difference between the structural behavior simulated by a fiber macroelement model and an elastically supported model (Fig. 32).

The moment-rotation relation in the fiber macroelement (Fig. 33) as well as the stress-strain relation in the side (most loaded Fiber 1 – Fig. 19) for various values of *PGA* (Fig. 34) are shown.

Unlike in the macroelement fiber model developed on the basis of Sofia sand soil conditions in the one developed on the basis of Sofia clay soil conditions the superstructure's behavior is with guiding importance. This is demonstrated by the occurrence of plastic hinges in the frame joints at values of *PGA* larger than 0.90*g*. At *PGA* = 1.50*g* a roughly simultaneous failure of column C4 and soil is observed (Fig. 35).

9. CONCLUSIONS

This paper has demonstrated the practical implementation of the macroelement fiber model for addressing soil-shallow foundation-superstructure interaction in nonlinear seismic analysis. A comprehensive example showcasing the application of the macroelement in commercial software has yielded promising results. The outcomes of nonlinear dynamic analysis underscore the efficacy of incorporating the fiber macroelement into well-established programs, providing a satisfactory consideration of soil-shallow foundation-superstructure interaction during seismic excitation.

Furthermore, the comprehensive discussion and findings presented in this paper emphasize the crucial significance of accounting for soil conditions in seismic numerical analysis. Neglecting this aspect can result in a profound misunderstanding of the actual structural behavior. The macroelement fiber model, as proposed in this study, offers a practical and suitable approach to rectify this issue, enhancing the accuracy and reliability of seismic analysis in structural engineering practice. It serves as a valuable tool to ensure that the influence of soil conditions is adequately addressed, thereby contributing to safer and more robust structural designs in seismic-prone regions.

REFERENCES

1. Powell, G. H., S. Campbell, 1994. *DRAIN-3DX element description and user guide for element type 01, type 04, type05, type 08, type 09, type 15, type 17, version 1.10*. Report No.UCB/SEMM-94/08.
2. Taucer, A., E. Spacone, F. Filippou, 1991. *A Fiber Beam-Column Element for Seismic Response Analysis of Reinforced Concrete Structures, Report UCB/EERC91-17*. Berkley: University of California.
3. Architectural Institute of Japan, 2001. *Recommendation for Design of Building Foundations (in Japanese).* Tokyo: AIJ.
4. Wilson, E. L., 2012. *Three-Dimensional Static and Dynamic Analysis of Structures - A Physical Approach with Emphasis on Earthquake Engineering*. California: CSI.
5. Storie, B., M. Pender, 2013. *SFSI in shallow foundation earthquake response*. Wellington, Proc. Annual Conference of the NZSEE.
6. Mair, R. J., 1993. Unwin memorial lecture 1992. Developments in geotechnical engineering research: application to tunnels and deep excavation. *Proceedings of the ICE —Civil Engineering*, 97(1), p. 27–41.
7. European Committee for Standardization, 2004. *Eurocode 8: Design provisions for earthquake resistance of structures - Part 5: Foundations, retaining structures and geotechnical aspects*. Brussels
8. Japanese Geotechnical Society, 1998. *Remedial Measures Against Soil Liquefaction*. Rotterdam: A. A. Balkema.

9. Gazetas, G., R. Dobry, J. L. Tassoulas, 1985. Vertical response of arbitrarily shaped embedded foundations. *Proc. ASCE Jnl. Geotech. Eng*, 111(6), p. 750-771.
10. Brinch Hansen, J., 1963. Discussion on Hyperbolic Stress-Strain Response. *Journal for Soil Mechanics and Foundation Engineering (ASCE)*, 97(6), pp. 931-932.
11. Milev, N., 2016. *Soil structure interaction – PhD Thesis (in Bulgarian)*. Sofia: UACEG.
12. Milev, Y., 2012. *Eurocode 8 – Seismic design of RC structures (Part I) (in Bulgarian)*. Sofia: Chamber of Engineers in the Investment Design.
13. Computers and Structures Inc, 2015. *ETABS Structural Software for Building Analysis and Design. Berkeley, California: CSI*.
14. Federal Emergency Management Agency, 2000. Prestandard and Commentary for the Seismic Rehabilitation of Buildings – FEMA 356. s.l.: Washington D.C.

USVAJANJE FIBER MAKROELEMENTA ZA RAČUNANJE EFEKTA SSI U ANALIZI NESAGLASNOG SEIZMIČKOG PONAŠANJA

Glavni cilj ovog rada je predložiti praktičan pristup za razmatranje efekta interakcije tla – plitke temeljne konstrukcije – nadgradnje u nelinearnoj seizmičkoj analizi. Interakcija tla i konstrukcije je komplikovan zadatak koji se bavi različitim inženjerskim problemima. Razmatranje efekta interakcije tla i konstrukcije proteže se izvan numeričke analize, geotehničkog istraživanja ili oblasti projektovanja konstrukcija. Veština razmatranja efekta interakcije tla i konstrukcije leži u ravnoteži između uključivanja uslova tla i nadgradnje u jedan zajednički model. Prateći ovu metodologiju uz klasične principe mehanike tla pruža dodatno poverenje inženjerskoj zajednici u usvajanje potpunog praktičnog koncepta. Ovaj rad predstavlja fiber makroelement koji predstavlja tlo ispod plitkih temelja. Ovo omogućava direktnu primenu fiber makroelementa u nelinearnoj analizi pomaka i dinamici u komercijalnim softverskim rešenjima, kao i jednostavnu primenu u otvorenim softverskim sistemima. Uvođenje procedure za formiranje matrice krutosti ovog elementa i modela histerezije tla takođe je ključni komponent. Posebna pažnja se posvećuje dobijanju krive osnovnih karakteristika materijala putem eksperimentalnih rezultata i procedura Evrokoda 8. Osim toga, ovaj rad demonstrira primenu makroelementa za razmatranje efekta interakcije tla i konstrukcije u nelinearnoj seizmičkoj analizi unutar komercijalnih softverskih rešenja. Glavni cilj je pružiti projektantima konstrukcija jednostavan pristup za uključivanje uslova tla u analizu nadgradnje. Rezultati numeričke analize na primeru zgrade sa konstrukcijom od armiranog betona u komercijalnom softveru ističu značaj ne potcenjivanja uslova tla. Ovaj rad naglašava da se oslanjanje isključivo na fiksne modele u svakodnevnom projektovanju konstrukcija može dovesti do opasnih i neočekivanih posledica.

Ključne reči: *makromodel, element vlakana, interakcija tla i konstrukcije, dinamika tla, likvefakcija, krivulja osnovnih karakteristika tla, degradacija krutosti, model histerezije, Evrokod 8*